Condensed Matter Physics.
Physics of thin films.
Surfaces and interfaces

UDC 538.956

EDN PVLCLE
https://www.doi.org/10.33910/2687-153X-2024-5-4-177-186

Dielectric properties of thin-film metal/dielectric nanocomposites based on zirconium nitrides

A. A. Galiullin ✉[1], I. V. Lunev [1], A. I. Gumarov [1], I. V. Yanilkin [1]

[1] Kazan Federal University, 18 Kremlyovskaya Str., Kazan 420008, Russia

Authors

Artur A. Galiullin, ORCID: 0000-0002-4872-1486, e-mail: www.ag95@mail.ru

Ivan V. Lunev, ORCID: 0000-0001-6201-4393, e-mail: lounev75@mail.ru

Amir I. Gumarov, ORCID: 0000-0002-7250-4377, e-mail: amir@gumarov.ru

Igor V. Yanilkin, ORCID: 0000-0002-8879-8904, e-mail: yanilkin-igor@yandex.ru

For citation: Galiullin, A. A., Lunev, I. V., Gumarov, A. I., Yanilkin, I. V. (2024) Dielectric properties of thin-film metal/dielectric nanocomposites based on zirconium nitrides. *Physics of Complex Systems*, 5 (4), 177–186. https://www.doi.org/10.33910/2687-153X-2024-5-4-177-186 EDN PVLCLE

Received 5 September 2024; reviewed 11 October 2024; accepted 11 October 2024.

Funding: This research was supported by the grant allocated to Kazan Federal University as part of the state-commissioned research assignment (project number FZSM-2023-0012).

Abstract. Zirconium oxynitride films were synthesized by sputtering zirconium nitride with subsequent atmospheric annealing to oxynitride. The resulting films were studied by dielectric spectroscopy. It was shown that the annealing temperature affects the dielectric properties of the film. Atmospheric annealing leads to dispersion of the permittivity and relaxation processes. The nonlinear nature of the temperature dependence of the relaxation time and the difference in the relaxation times are manifestations of the heterogeneous structure of the films and the size effect of the metal/dielectric structure.

Keywords: heterogeneous materials, dielectric spectroscopy, dielectric relaxation, zirconium oxynitrides, thin films

Introduction

Thin-film metal-dielectric composites based on transition metal nitrides are of considerable interest to photonics. In their pure form, they are modern plasmonic materials with an advantage over traditional silver, gold, and copper. This advantage is refractoriness. They play a significant role in such dynamic fields as telecommunications, information processing and storage, quantum information technologies, and spectroscopy.

The literature analysis has shown that zirconium oxynitride films are usually synthesized by reactive magnetron sputtering in a mixture of argon (active gas), oxygen, and nitrogen (reactive gases) (Carvalho et al. 2008; Courts, Swinehart 2003). In this case, the key parameter determining the resistive properties of the film is the ratio of the fractions of active and reactive gases.

Resistance thermometers (RTD) are commercially available and are made on the basis of ruthenium dioxide, rhenium oxide, rhodium with the addition of iron, platinum, zirconium nitride and oxynitride, germanium. They also include silicon and aluminum gallium arsenide diodes (Carvalho et al. 2008; Mohamed et al. 2015). The main difference between all these materials is the operating temperature range.

Heat treatment of zirconium oxynitride in air directly affects its physical properties. The effect of heat treatment on zirconium oxynitride was studied by You, *et al.* (You et al. 2022). Annealing of the samples resulted in a decrease in the nitrogen content and a spontaneous increase in the oxygen content. A huge increase in specific electrical resistance was observed during oxidation. Films annealed at higher temperatures (≥ 723 K) showed insulating properties.

The effect that the regulation of the oxygen content has on the structure and properties of this type of film was studied by (Mohamed et al. 2015). Oxygen atoms replace nitrogen atoms, introduce a Zr vacancy into the ZrN structure, and lead to a phase transition from ZrN to Zr_3N_4. Even small changes in the oxygen content lead to an electronic transition from metallic to semiconductor behavior in the ZrN structure. (da Silva-Oliveira et al. 2018; Khan et al. 2017) investigated the effect of heat treatment on the structural, morphological and mechanical properties of zirconium oxynitride films.

(Streibel et al. 2024) investigated the applicability of zirconium oxynitride thin films as semiconductor photoanodes, as well as the effect of annealing on photoelectrochemical characteristics.

During this study, metal/dielectric composites based on zirconium oxynitride were synthesized. The study analyses and describes the dielectric properties of thin-film metal/dielectric nanocomposites based on nitrides in wide temperature and frequency ranges.

Materials and methods

The films were synthesized by reactive magnetron sputtering of zirconium onto single-crystal, 0001-oriented corundum substrates (Monocrystal, Russia). The substrate surfaces were prepared in several stages. After an ultrasonic bath in acetone (high purity grade) and isopropyl alcohol (high purity grade), they were annealed at 1073 K for 5 minutes in an ultrahigh vacuum chamber (SPECS, Germany) with a residual vacuum of ~ 2×10^{-10} mbar. After annealing, the sample was moved along an ultrahigh vacuum line into a magnetron sputtering chamber (BESTEC, Germany) with a residual gas pressure below 5×10^{9} mbar.

The magnetron operated in DC mode, the discharge power was 50 W, the target was a zirconium washer (99.5% purity, GIRMET Ltd, Russia), 5 mm thick and 5 cm in diameter. Zirconium oxynitride films were synthesized in two stages: 1) zirconium nitride sputtering; 2) annealing of the nitride film in air for one hour to obtain oxynitride. The annealing temperature critically affects the resistive properties of the film. To protect the films against further uncontrolled exposure to the atmosphere, they were covered with a 20 nm thick zirconium oxide film after preliminary cleaning with argon ions. The initial zirconium nitride film has a resistivity of 0.29 mOhm×m at 300 K, which is two orders of magnitude higher than typical values for ZrN films. This is due to the presence of oxygen in the film, amounting to 15 at.%. The resistivity of zirconium oxynitride films annealed in air increases and is determined by the annealing temperature (up to the dielectric state), which is associated with an increase in the proportion of the oxide phase in the composite.

High-purity argon (> 99.99%) was used as a plasma-forming gas at a pressure of 6×10^{-3} mbar. For reactive spraying of nitride or zirconium oxide, nitrogen or oxygen (both gases with purity > 99.99%) were additionally introduced into the chamber, respectively, while maintaining the operating pressure unchanged. This gas purity (1 ppm) is achieved through the use of fine filters (PerkinElmer). The filter system is integrated into the gas aftertreatment stand through which all gases used in spraying experiments are filtered. When spraying zirconium nitride, the substrate was maintained at a temperature of 573 K, when spraying the oxide, at room temperature. To determine the spraying mode, the deposition rate was measured on a quartz thickness gauge (INFICON) depending on the composition of the plasma-forming gas. As a result, a concentration of about 3.9% was selected for both reactive gases, which corresponds to the spraying of the oxidized target surface ('oxidized' mode). The deposition rate of zirconium nitride was 1.5 nm/min, while it was 0.9 nm/min for zirconium oxide.

The electrical properties of the samples were studied using the dielectric spectroscopy on the Novocontrol Concept BDS-80 broadband measuring complex. Electrical characteristics were measured in the frequency range from 10^{-1} Hz to 10^{7} Hz and the temperature range from 123 to 473 K, with a step of 5 K.

The sample under study is located in the measuring cell (a plane-parallel capacitor), which is placed in the measuring head. During the measurements, the head is immersed in a cryothermostat chamber connected to a gaseous nitrogen supply line from the cooling system. The cooling rate is regulated by a programmable system for supplying gaseous nitrogen from a Dewar vessel due to the evaporation of liquid nitrogen. A temperature sensor with an accuracy of ± 0.1 K is connected to the measuring head.

See Supplementary Materials (Figure S1) for the temperature protocol for the dielectric measurements.

 https://www.doi.org/10.33910/2687-153X-2024-5-4-177-186

The studied sample was cooled to a temperature of 123 K. After the temperature stabilized, the dielectric spectrum was measured. Then the temperature was increased by 5 K, stabilized, and the next measurement was carried out. Upon reaching a temperature of 473 K and measuring the dielectric spectrum, the experiment was completed.

Samples of ZrON metal-dielectric films on a dielectric substrate Al_2O_3 were studied. The substrate and film samples with different temperatures of annealing were measured separately. The characteristics of the samples are given in Table 1.

Table 1. Characteristics of the studied ZrON-based samples

Sample	Thickness, mm	Annealing time, h	Annealing temperature, K
Al_2O_3 substrate	0.66	–	–
ZrN	0.660123	–	–
ZrON_573	0.660123	1	573
ZrON_623	0.660123	1	623

Results

Al_2O_3 substrate

Figure 1a shows the real part of the permittivity of the corundum substrate.

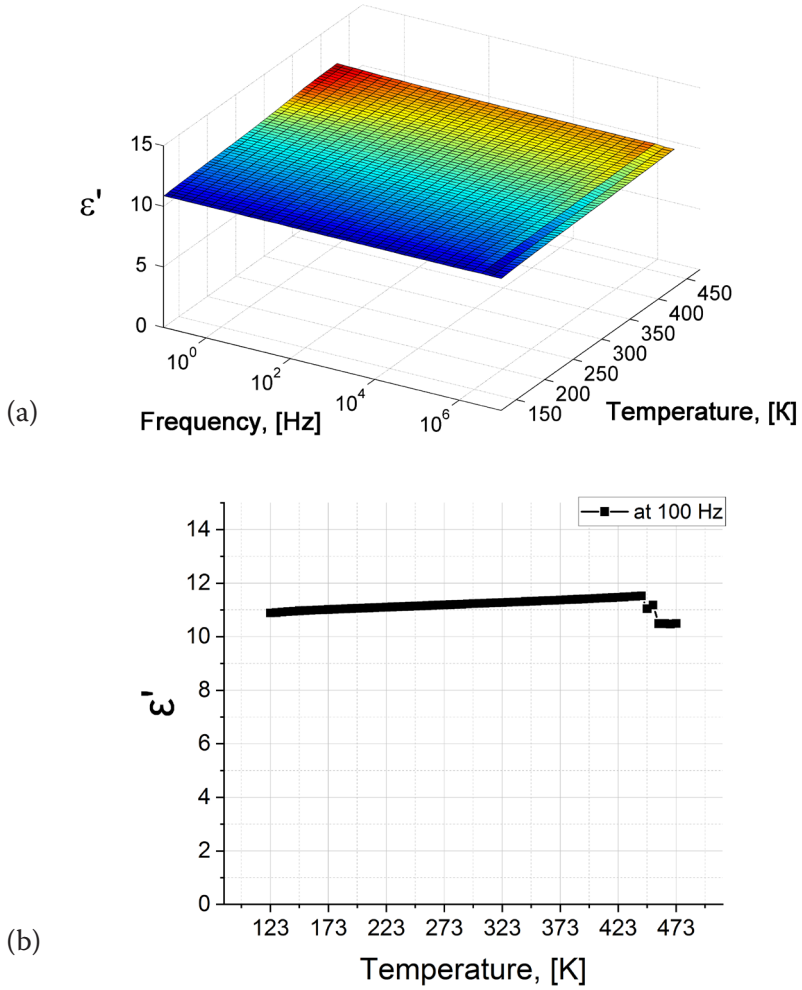

Fig. 1. 3D diagram in (f, T, ε') coordinates (a) and temperature dependence at a frequency of 100 Hz (b) of the real part of the permittivity of the Al_2O_3 substrate

The substrate demonstrates good dielectric properties, the real part of the permittivity increases linearly with increasing temperature (Figure 1b). At temperatures above 443 K there is some instability, probably related to the measurement technique.

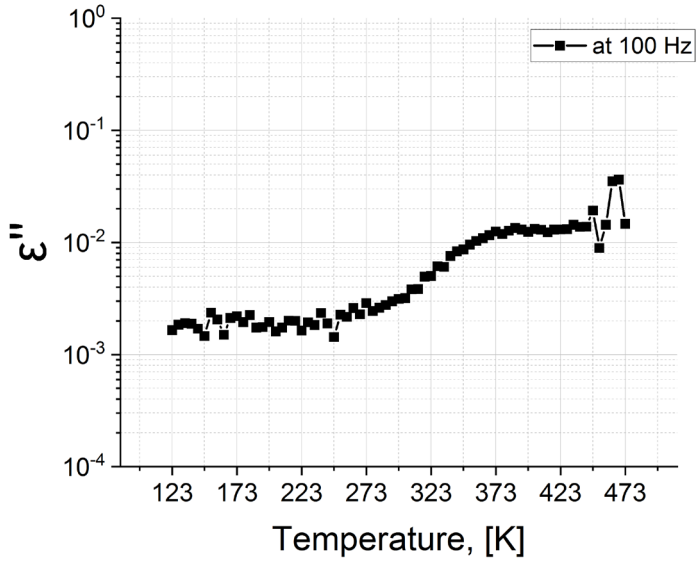

Fig. 2. Temperature dependence of the imaginary part of the permittivity of the Al_2O_3 substrate at a frequency of 100 Hz

No relaxation processes are observed in the entire temperature range. At a temperature of 293 K, the permittivity ε' equals to 11.2, dielectric losses $\varepsilon'' = 0.003$ (Figure 2).

ZrN film on the substrate without annealing

Figures 3a and 3b show three-dimensional diagrams of the real and imaginary parts of the permittivity of the ZrN film on the substrate without annealing. At a temperature of about 350 K, a local increase in the permittivity value is observed. This may be due to structural defects in the deposited film.

In direct current mode the ZrN film shows metallic properties and has a specific resistance of 0.29 mOhm×m, although dielectric properties are manifested on alternating current in the frequency range of 10^3–10^7 Hz. Therefore, it was possible to measure the dielectric characteristics in the specified frequency range. The sample has a through conductivity of $\sigma_0 = 2.5 \times 10^{-5}$ Sm×m^{-1} at a temperature of 293 K. It might be due to the film material getting onto the edges of the substrate during the synthesis.

Figure 4 shows the temperature dependence of the permittivity of the ZrN film determined at a frequency of 1 kHz. In the temperature range of 348–373 K, uneven behavior of ε' and ε'' is observed. This is probably due to the heterogeneous composition of the sample.

ZrON film after annealing at a temperature of 573 K

Figures 5a and 5b show 3D diagrams of the real and imaginary parts of the permittivity of the ZrON_573 sample.

A relaxation process is observed in the entire temperature range of 123–473 K (Figure 5b). The increase in amplitude in the frequency range of 10^{-1}–10^2 Hz in the temperature range of 300–473 K (Figure 5a) is associated with the manifestation of electrode polarization.

The relaxation process in the obtained spectra was approximated by superposition of the Cole-Cole function (Cole, Cole 1941) and Jonscher function:

$$\varepsilon^*(\omega) = \varepsilon'(\omega) - i\varepsilon''(\omega) = \varepsilon_\infty + \frac{\Delta\varepsilon}{1+(i\omega\tau)^\alpha} + B(i\omega)^{n-1}, \quad (1)$$

ε' and ε'' denotes the real and imaginary parts of the complex permittivity, $\omega = 2\times\pi\times f$ is the cyclic frequency. The parameter ε_∞ denotes the extrapolated high-frequency permittivity, and $\Delta\varepsilon = \varepsilon_s - \varepsilon_\infty$ is the relaxation amplitude (the permittivity low-frequency limit is denoted by ε_s). The parameter τ is the

 https://www.doi.org/10.33910/2687-153X-2024-5-4-177-186

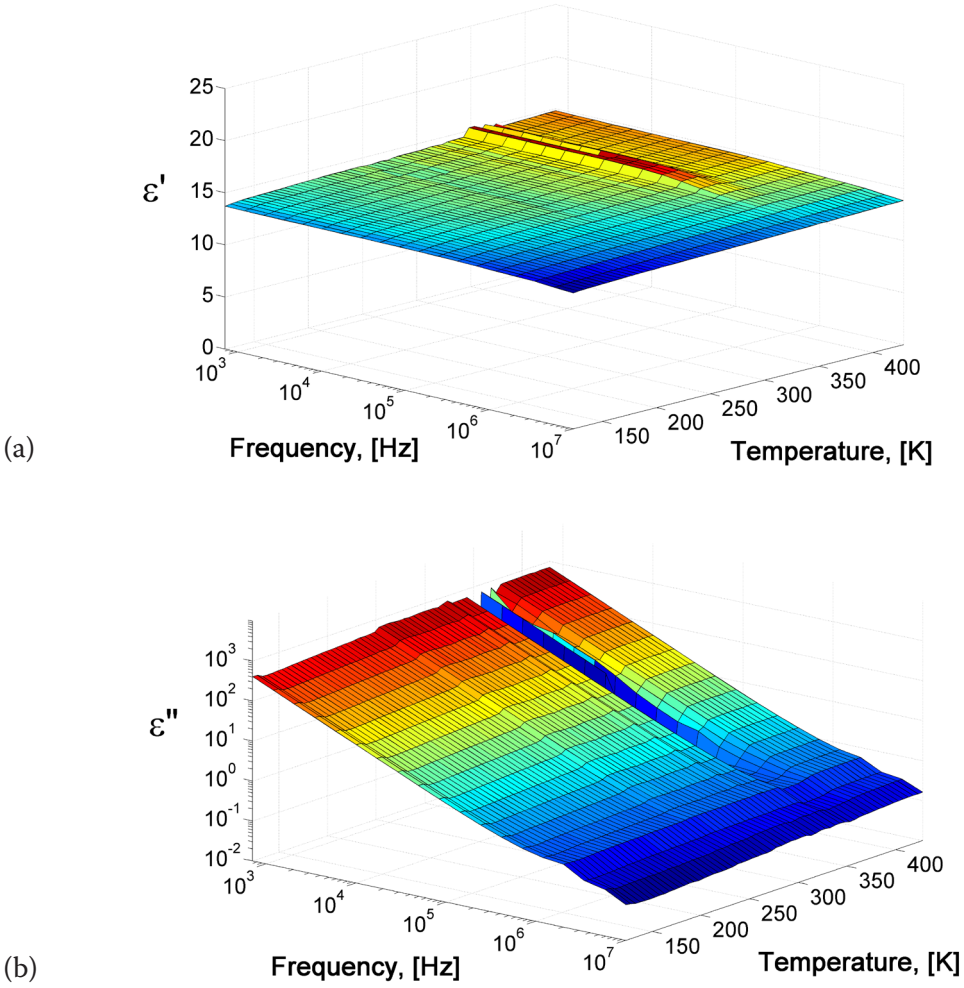

Fig. 3. 3D diagrams of the real (a) and imaginary (b) parts of the permittivity of the ZrN film on the substrate without annealing

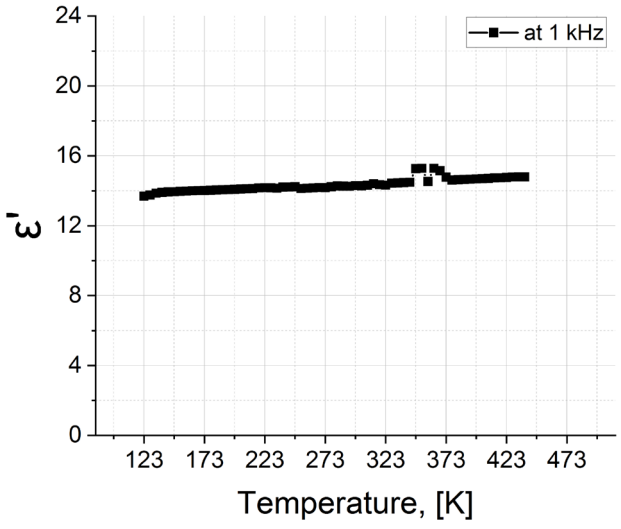

Fig. 4. Temperature dependence of the real part of the permittivity of the ZrN film

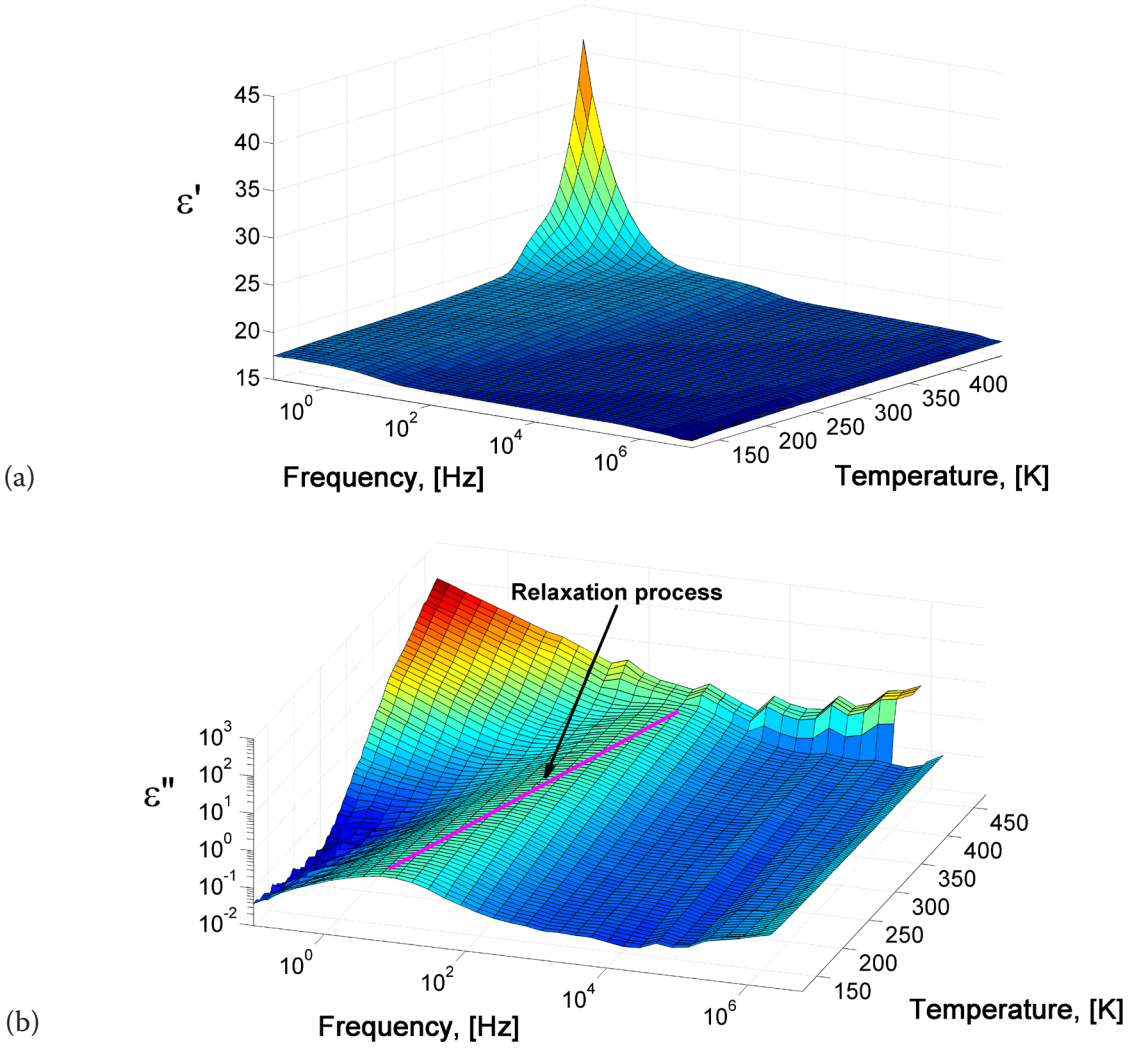

Fig. 5. 3D diagrams of the real (a) and imaginary (b) parts of the permittivity of the ZrON_573 sample

relaxation time. The exponent α ($0 < \alpha \leq 1$) is a measure of the symmetric broadening of the spectrum. The Jonscher function takes into account electrode effects. B is the contribution of the Jonscher function, $0 < n \leq 1$ is the function parameter.

ZrON film after annealing at 623 K

Figures 6a and 6b show 3D diagrams of the real and imaginary parts of the permittivity of the ZrON_623 sample. The relaxation process is observed in the entire temperature range of 123–473 K.

The relaxation process under consideration is described by formula (1). The increase in amplitude in the frequency range of 10^{-1}–10^{2} Hz in the temperature range of 300–473 K (Figure 10 and 11) is associated with the manifestation of the effect of electrode polarization.

Discussion

As a result of measuring the electrical properties of the samples indicated in Table 1 in the frequency range of 10^{-1}–10^{7} Hz and the temperature range of 123–473 K, the dielectric characteristics, permittivity ε' and relaxation time τ were determined, using formula (1).

Figure 7 shows the temperature dependences of permittivity ε'.

From Figure 7 it is evident that upon application of the ZrN film onto the Al_2O_3 substrate and its subsequent oxidation, the permittivity of the samples increases. If we consider the values of ε' at a temperature of 300 K, it is evident that ε' increases. For the substrate, ε' equals 11.2. After application of the ZrN film, the permittivity increases to a value of $\varepsilon' = 14.3$. After annealing at a temperature of 573 K for

 https://www.doi.org/10.33910/2687-153X-2024-5-4-177-186

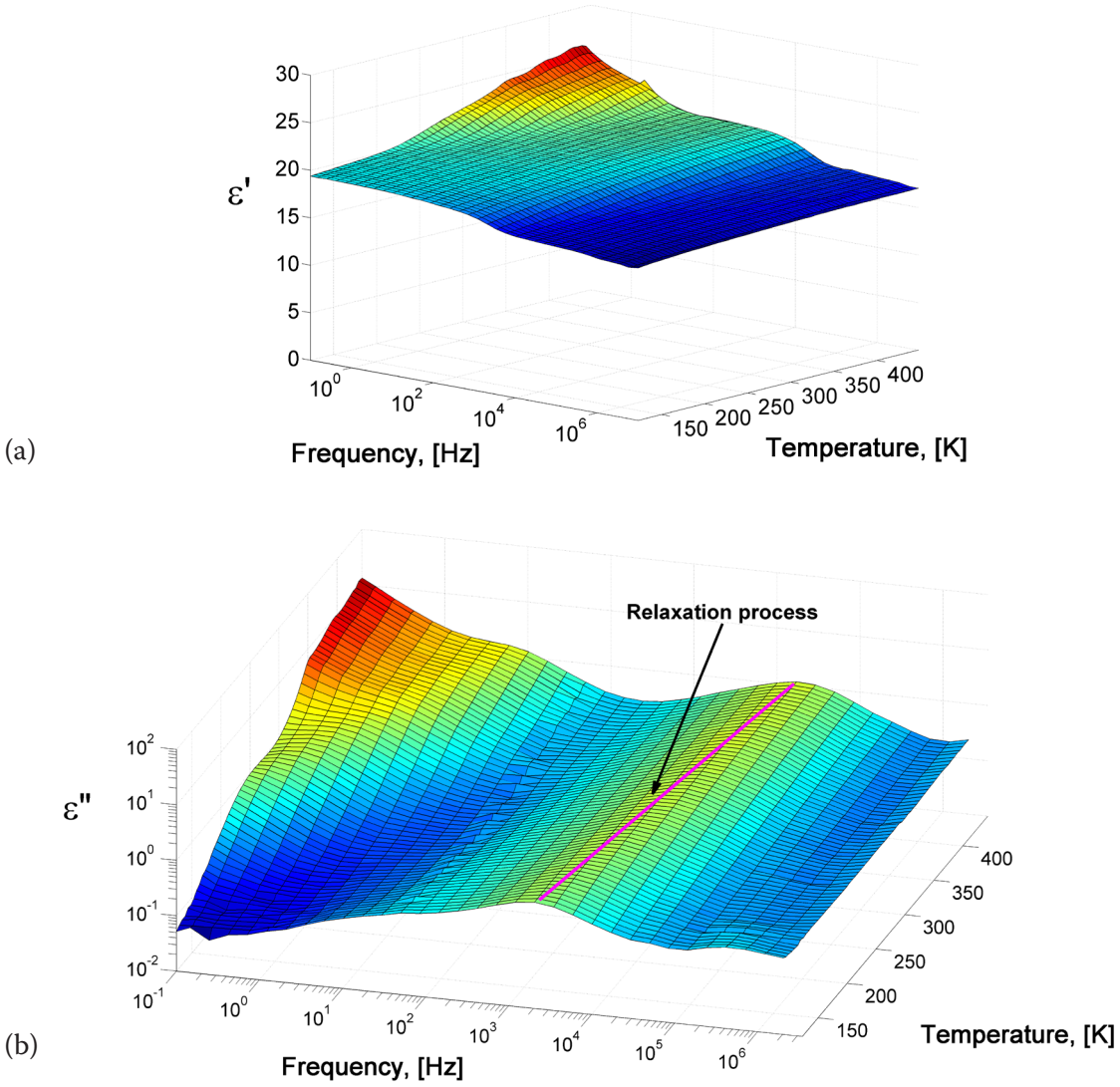

Fig. 6. 3D diagrams of the real (a) and imaginary (b) parts of the permittivity of the ZrON_623 sample in (f, T, ε′) coordinates

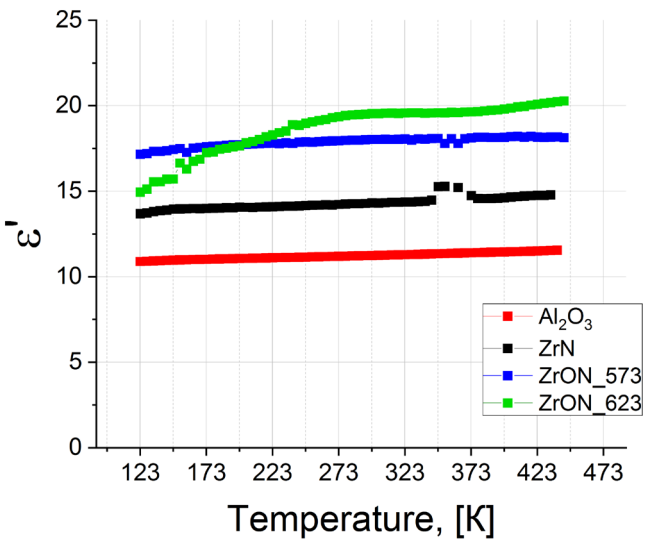

Fig. 7. Temperature dependence of the permittivity of the studied samples

one hour, the permittivity increases and has a value of $\varepsilon' = 18$. With further oxidation and annealing of the ZrN foam sample on the Al_2O_3 substrate for one hour at a temperature of 623 K, the permittivity value $\varepsilon' = 19.5$. For the ZrON_623 sample, the temperature dependence of $\varepsilon'(T)$ is non-uniform; in the temperature range of 123–300 K, it rapidly increases from 14.9 at 123 K to 19.5 at 300 K, then increases more smoothly with increasing temperature. Apparently, this is the way the heterogeneous structure of the ZrON_623 sample becomes manifest: it increases with increasing annealing temperature.

Figure 8 shows the temperature dependences of the relaxation time τ and processes detected in the ZrON_573 and ZrON_623 samples, in Arrhenius coordinates.

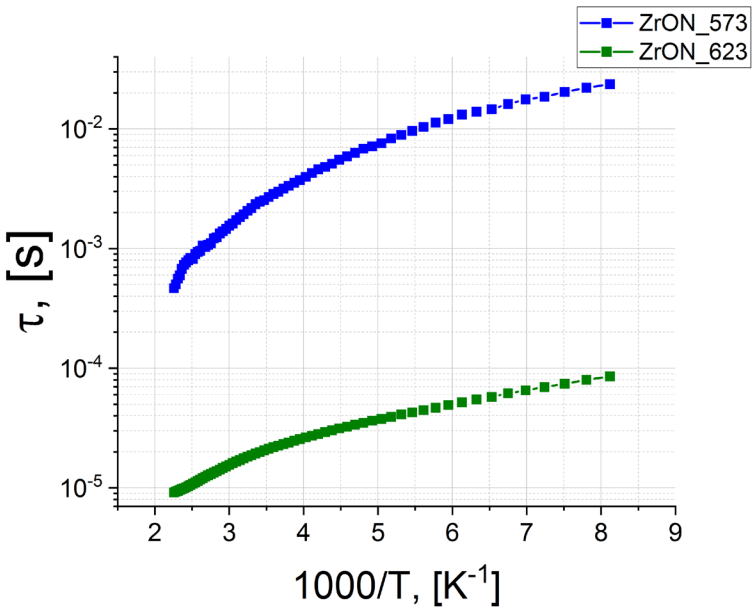

Fig. 8. Temperature dependence of the relaxation time τ of the ZrON_573 and ZrON_623 samples in Arrhenius coordinates

As was said earlier, no relaxation processes were observed in the ZrN substrate and film samples. Relaxation processes became manifest in the oxidized samples. The τ *(1000/T)* dependencies are non-linear (Figure 8). The ZrON_573 sample is characterized by longer relaxation times. The ZrON_623 sample has shorter relaxation times compared to ZrON_573. Apparently, during oxidation of zirconium due to atmospheric annealing, a change in the film structure occurs with the formation of dielectric regions. An increase in the annealing temperature leads to an increase in the number of dielectric regions and a wider distribution of their sizes, as well as an increase in the rate of charge exchange, which leads to a decrease in the relaxation time.

The mechanism by which dielectric dispersion occurs is as follows. The synthesized film has a metallic type of conductivity, that is, electrons transfer the charge, and there is no dielectric dispersion. The film under study has a polycrystalline granular structure. During atmospheric annealing, oxygen penetrates into the space between the grains, oxidizing particles of zirconium nitride ZrN to zirconium oxynitride ZrON, which is a dielectric. Thus, the film is transformed into a metal-dielectric composite. Dielectric particles are a kind of defect in the film structure that limits the mobility of electrons. This leads to the localization of electrons near defects for some time and the appearance of an additional dipole moment, which, in turn, leads to dispersion of the permittivity and the emergence of relaxation processes. An increase in the annealing temperature leads to an increase in the number of dielectric regions and a wider distribution of their sizes, as well as an increase in the rate of charge exchange, which leads to a decrease in relaxation time.

Conclusions

The reported study identified the effect of annealing temperature on the dielectric properties of a zirconium oxynitride film synthesized by zirconium nitride sputtering, followed by atmospheric annealing and the formation of oxynitride. An increase in the permittivity from 14.3 to 18 and 19.5 at a temperature

 https://www.doi.org/10.33910/2687-153X-2024-5-4-177-186

of 300 K was shown for the initial samples and those annealed at temperatures of 573 and 623 K, respectively. Atmospheric annealing leads to a dispersion of the permittivity and relaxation processes. For the samples annealed at a temperature of 573 and 623 K, the temperature dependencies of the relaxation times are nonlinear in Arrhenius coordinates and differ by almost two orders of magnitude. For example, at a temperature of 300 K, the values are 2.3×10^{-3} and 1.9×10^{-5} s, respectively. The nonlinear nature of the temperature dependence of the relaxation time and the difference in the relaxation times for samples annealed at a temperature of 573 and 623 K is a manifestation of their heterogeneous structure and the size effect of the metal/dielectric structure.

Supplementary Materials

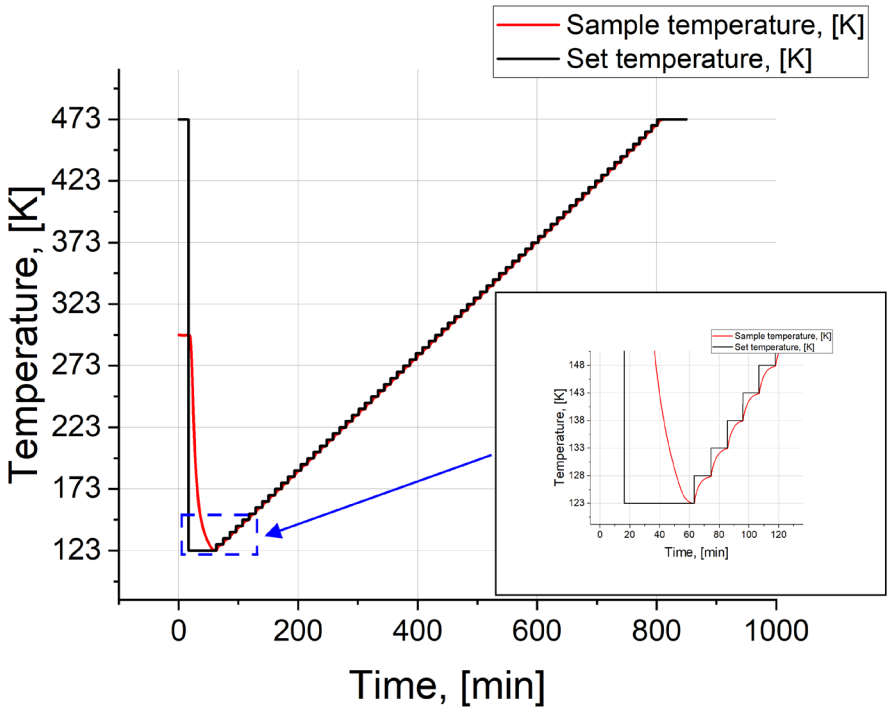

Fig. S1. Temperature protocol of dielectric measurements

Conflict of Interest

The authors declare that there is no conflict of interest, either existing or potential

Author Contributions

I. V. Lunev, A. A. Galiullin — investigation, visualization, writing, metodology; A. I. Gumarov, I. V. Yanilkin — resources.

References

Carvalho, P., Chappé, J. M., Cunha, L. et al. (2008) Influence of the chemical and electronic structure on the electrical behavior of zirconium oxynitride films. *Journal of Applied Physics*, 103 (10), article 104907. https://doi.org/10.1063/1.2927494 (In English)

Cole, K. S., Cole, R. H. (1941) Dispersion and absorption in dielectrics I. Alternating current characteristics. *The Journal of Chemical Physics*, 9 (4), 341–351. https://doi.org/10.1063/1.1750906 (In English)

Courts, S. S., Swinehart, P. R. (2003) Review of Cernox™ (zirconium oxy-nitride) thin-film resistance temperature sensors. *AIP Conference Proceedings*, 684 (1), 393–398. https://doi.org/10.1063/1.1627157 (In English)

Da Silva-Oliveira, C. I., Martínez-Martínez, D., Apreutesei, M. et al. (2018) Thermal stability of Zr-O-N(:Ti) thin films prepared by magnetron sputtering. *Vacuum*, 151, 148–155. https://doi.org/10.1016/j.vacuum.2018.02.002 (In English)

Khan, I. A., Kashif, M., Farid, A. et al. (2017) Effect of annealing temperature on the structural, morphological, and mechanical properties of polycrystalline zirconium oxynitride composite films deposited by plasma focus device. *Japanese Journal of Applied Physics*, 56 (12), article 125501. https://doi.org/10.7567/JJAP.56.125501 (In English)

Mohamed, S. H., Hadia, N. M. A., Ali, H. M. (2015) Effect of annealing on properties of decorative zirconium oxynitride thin films. *European Physical Journal Applied Physics*, 69 (3), article 30301. https://doi.org/10.1051/epjap/2015140475 (In English)

Streibel, V., Schönecker, J. L., Wagner, L. I. et al. (2024) Zirconium oxynitride thin films for photoelectrochemical water splitting. *ACS Applied Energy Materials*, 7 (9), 4004–4015. https://doi.org/10.1021/acsaem.4c00303 (In English)

You, M., Li, Y., Zhang, H. et al. (2022) The mechanism of phase transition induced by oxygen doping in zirconium nitride thin films. *Journal of Materials Science*, 57 (4), 18456–18467. https://doi.org/10.1007/s10853-022-07182-z (In English)